Glycogenic activity of R6, a protein phosphatase 1 regulatory subunit, is modulated by the laforin-malin complex

Carla Rubio-Villena, Maria Adelaida Garcia-Gimeno[$] and Pascual Sanz*[$]

Instituto de Biomedicina de Valencia, CSIC, and Centro de Investigación en Red de Enfermedades Raras (CIBERER), Jaime Roig 11, 46010-Valencia, Spain.

[$]These two senior authors contributed equally to this work.

*Corresponding author: Dr. Pascual Sanz, Instituto de Biomedicina de Valencia, CSIC, Jaime Roig 11, 46010-Valencia, Spain. Tel: +34963391779; FAX: +34963690800;
e-mail: sanz@ibv.csic.es

Short title: R6-PP1 glycogenic subunit is downregulated by the laforin-malin complex

ABSTRACT

Protein phosphatase type 1 (PP1) plays a major role in the regulation of glycogen biosynthesis. PP1 is recruited to sites of glycogen formation by its binding to specific targeting subunits. There, it dephosphorylates different enzymes involved in glycogen homeostasis leading to an activation of glycogen biosynthesis. Regulation of these targeting subunits is crucial, as excess of them leads to an enhancement of the action of PP1, which results in glycogen accumulation. In this work we present evidence that PPP1R3D (R6), one of the PP1 glycogenic targeting subunits, interacts physically with laforin, a glucan phosphatase involved in Lafora disease, a fatal type of progressive myoclonus epilepsy. Binding of R6 to laforin allows the ubiquitination of R6 by the E3-ubiquitin ligase malin, what targets R6 for autophagic degradation. As a result of the action of the laforin-malin complex on R6, its glycogenic activity is downregulated. Since R6 is expressed in brain, our results suggest that the laforin-malin complex downregulates the glycogenic activity of R6 present in neuron cells to prevent glycogen accumulation.

Abbreviations: AMPK, AMP-activated protein kinase; GAD, Gal4 activating domain; GS, glycogen synthase; LD, Lafora disease; PKA, protein kinase A; Ph, glycogen phosphorylase.

1. INTRODUCTION

Protein phosphatase 1 (PP1) is a serine/threonine protein phosphatase which plays important roles in the regulation of a broad range of physiological processes, including cell proliferation, differentiation, survival and death (Heroes et al. , 2012). In the later years it has become evident that free PP1 has essentially no specificity for substrates, its specificity being regulated by more than 200 PP1-interacting proteins (PIPs), which create a vast variety of PP1 holoenzymes with a distinct subset of substrates and mechanisms of regulation (Bollen et al. , 2010, Heroes, Lesage, 2012). One of the processes regulated by PP1 is glycogen homeostasis. In this case, PP1 interacts with a specific set of glycogen targeting subunits which contain a carbohydrate binding module of the CBM21 type. Seven recognized glycogen targeting subunits have been identified, namely PPP1R3A (GM), PPP1R3B (GL), PPP1R3C (R5/PTG), PPP1R3D (R6), PPP1R3E (R3E), PPP1R3F (R3F) and PPP1R3G (R3G) (in brackets, the informal name) (Heroes, Lesage, 2012). These subunits target PP1 to specific enzymes involved in glycogen homeostasis: they bind glycogen synthase (GS), allowing in this way the dephosphorylation of the synthase and its activation; they also bind glycogen phosphorylase (Ph) and glycogen phosphorylase kinase (PhK), allowing the dephosphorylation and inactivation of these enzymes. In this way the net action of PP1 on glycogen homeostasis is to improve glycogen accumulation, since it promotes the synthesis of the polysaccharide and prevents its degradation (Roach et al. , 2012). Although these subunits bind to PP1 through a similar RVxF docking motif, they are

structurally different and more importantly, their function is regulated by different mechanisms depending on the corresponding subunit. For example, the activity of GM is regulated by phosphorylation of the subunit by PKA, whereas the activity of GL is inhibited allosterically by the binding of Ph to the C-terminus of the regulatory subunit (Roach, Depaoli-Roach, 2012).

The PP1-PPP1R3X holoenzymes play a main role in glucose homeostasis since they regulate glycogen synthesis and degradation in key tissues such as liver and skeletal muscle. In addition, the participation of R5/PTG in the regulation of glycogen synthesis in the neurons has been described recently. In fact, enhancement of R5/PTG function leads to the accumulation of insoluble polyglucosans in neuronal cells (Vilchez et al. , 2007), and R5/PTG is associated with a fatal type of progressive myoclonus epilepsy named Lafora disease (LD, OMIM 254780). This disease is produced by mutations in either the EPM2A gene, encoding the glucan phosphatase laforin, or the EPM2B gene, encoding the E3-ubiquitin ligase malin. These two proteins form a functional complex and defects in any of them lead to the disease, which correlates with the appearance of poorly-branched insoluble polyglucosans named Lafora bodies. It has been proposed that the laforin-malin complex interacts with R5/PTG and ubiquitinates it, impairing its glycogenic activity [(Vilchez, Ros, 2007), (Solaz-Fuster et al. , 2008), (Worby et al. , 2008)]. In addition, we have recently reported that the key metabolic sensor AMP-activated protein kinase (AMPK), on one hand enhances the function of the laforin-malin complex, and on the other hand, it is able to phosphorylate R5/PTG, facilitating in this way the recognition of this subunit by the laforin-malin complex and its ubiquitination [(Solaz-Fuster, Gimeno-Alcaniz, 2008), (Vernia et al. , 2009)].

Very little is known about the mechanism of regulation of R6 (PPP1R3D) activity. Since R6 is expressed in brain [(Armstrong et al. , 1997), (Esteves et al. , 2012)], this subunit could also have a role in regulating glycogen synthesis in this organ. For this reason we analyze the glycogenic activity of this subunit and whether the activity of R6 could also be regulated by the laforin-malin complex. In this work we present evidence of a physical interaction between laforin and R6. This interaction leads to the malin-dependent ubiquitination of R6, which is targeted for autophagic degradation. Using a neuronal cell model (Neuro-2a), we also show that R6, laforin, malin and glycogen synthase are located in similar cytosolic areas of the cell, revealing a common role of these proteins on the regulation of glycogen homeostasis in this neuronal cell type.

2. MATERIALS AND METHODS

2.1. Plasmids. pCMV-HA-laforin, pcDNA3-HA-malin and pFlag-R6 constructs were described previously [(Solaz-Fuster, Gimeno-Alcaniz, 2008), (Garcia-Haro et al. , 2010)]. pBTM-R6 and pGADT7-R6 plasmids were obtained by digesting a R6 plasmid (Worby, Gentry, 2008) with EcoRI/XhoI and subcloning the fragment containing the R6 open reading frame (ORF) into pBTM116 (EcoRI/SalI) or pGADT7 plasmids, respectively. Plasmid pEYFP-R6 was obtained by digesting plasmid pGADT7-R6 with HindIII/KpnI and subcloning the resulting fragment into pEYFP-C1 (BD Biosciences, Madrid, Spain). Plasmid pCMV-myc-R6 was obtained by digesting pGADT7-R6 with SfiI/XhoI and subcloning the resulting fragment into pCMVmyc (BD Biosciences, Madrid,

Spain). Other plasmids used in this study were pCMV-6xHisUbiq (from Dr. M. Rodriguez, Proteomics Unit, CIC-BioGUNE, Vizcaya, Spain); pCMV-6xHisUbiq K48R and pCMV-6xHisUbiq K63R (from Dr. Ch. Blattner, Institute of Toxicology and Genetics, Karlsruhe Institute of Technology, Karlsruhe, Germany); pCMV-Mdm2 [from Dr. M. Gentry, University of Kentucky, Lexington, KY; (Worby, Gentry, 2008)]; pCMV-6xHisHAUbiq KO was kindly provided by Dr. W. Gu [Institute of Cancer Genetics, Columbia University, New York, USA; (Li et al. , 2003)] and pCFP-laforin was a generous gift from Dr. Romá-Mateo (IBV-CSIC, Valencia, Spain).

2.2. Cell Culture, Transfection and Treatments. Murine neuroblastoma Neuro-2a (N2a) and human embryonic kidney (HEK-293) cells were grown in Dulbecco's modified Eagle's medium (Lonza, Barcelona, Spain), supplemented with 100 units/ml penicillin, 100 µg/ml streptomycin, 2 mM glutamine and 10% of inactivated fetal bovine serum (Invitrogen, Madrid, Spain) in a humidified atmosphere at 37ºC with 5% CO_2. Cells were transfected with 1 µg of each plasmid using X-treme GENE HP transfection reagent (Roche Diagnostics, Barcelona, Spain) according to the manufacturer's instructions. When indicated, eighteen hours after transfection, cells were treated with MG132 (25 µM), ammonium chloride (20 mM)/ leupeptin (100 µM) or lactacystin (5 µM) for 6 hours. Cell extracts were prepared using lysis buffer [25 mM Tris HCl at pH 7.4, 15 mM EDTA at pH 8, 50 mM NaF, 0.6 M sucrose, 15 mM 2-mercaptoethanol, 15 mM $Na_2P_2O_7$, 1 mM PMSF, and a complete Mini-EDTA free protease inhibitor mixture (Roche Diagnostics, Barcelona, Spain)]. Cells were lysed by repeated passage through 24Gx5/8'' needle. Twenty micrograms of total protein from the soluble fraction of cell lysates were analyzed by SDS-PAGE and Western blotting using appropriated antibodies: anti-myc, anti-Flag, anti-HA (Sigma-Aldrich, Madrid, Spain); anti-tubulin, anti-Mdm2, anti-LexA (Santa Cruz Biotechnology, Barcelona, Spain),

2.3. Yeast two-hybrid analysis. Yeast THY-AP4 strain [*MATα ura3 leu2 trp1 lexA::lacZ lexA::HIS3 lexA::ADE2*] (Paumi et al. , 2007) was transformed with plasmids pBTM-R6 (LexA-R6) and pACT2 (GAD, empty plasmid), pACT2-malin (GAD-malin) or pACT2-laforin (GAD-laforin), or with pGADT7-R6 (GAD-R6) and plasmids pBTM (LexA, empty plasmid), pBTM-malin (LexA-malin) or pEG202-laforin (LexA-laforin). Transformants were grown in selective SC medium, and β-galactosidase activity was assayed in permeabilized cells and expressed in Miller units as in (Ludin et al. , 1998).

2.4 Co-immunoprecipitation analysis. Neuro-2a cells were transfected with pCMV-HA-laforin and pCMV-myc-R6 or with the corresponding empty plasmids. Cells were scraped on ice in lysis buffer [50 mM Tris–HCl pH 8; 10 mM KCl, 50 mM EDTA; 15% glycerol, 1% nonidet P-40 (NP-40), complete protease inhibitor cocktail (Roche Diagnostics, Barcelona, Spain), 1 mM PMSF, 50 mM NaF, 2 mM $NaVO_4$ and 5 mM $Na_2P_2O_7$]. Cell lysis was performed as described above. Cell lysates were then centrifuged at 13,000x g for 15 min at 4ºC. R6-laforin complexes were immunoprecipitated from supernatants (500 µg of total protein) with anti-myc polyclonal antibody (Sigma-Aldrich, Madrid, Spain) and visualized by immunoblotting using anti-myc-HRP or anti-HA-HRP (Sigma-Aldrich, Madrid, Spain) antibodies.

2.5. Study of *in vivo* ubiquitination of R6. For ubiquitination assays, HEK-293 cells were co-transfected with pCMV-myc-R6, 6xHis-tagged ubiquitin plasmids and, when indicated, with pcDNA3-HA-malin and pCMV-HA-laforin plasmids, using X-treme GENE transfection reagent, according to the manufacturer's instructions (Roche Diagnostics, Barcelona, Spain). After 18 h of transfection, when indicated, cell were treated with MG132 (25 µM) for 6 hours. Then cells were lysed and ubiquitinated proteins purified by metal affinity chromatography (Kaiser and Tagwerker, 2005). Bound proteins and clarified extracts were analyzed by immunoblotting with the appropriated antibodies.

2.6. Glycogen determination. Neuro-2a transfected cells were scraped on ice into 30% KOH and then heated at 100ºC for 15 min. Glycogen was measured as described previously (Chan and Exton, 1976) and expressed as µg of glucose per mg of protein.

2.7. Immunofluorescence and confocal microscopy. Neuro-2a cells transfected with the indicated plasmids were grown on 12-well plates containing coverslips. Cells were fixed with 4% paraformaldehyde in phosphate-buffered saline (PBS) for 10 min. For direct fluorescence, cells were washed three times with PBS and stained with 4',6-diamidino-2-phenylindole (DAPI) for 10 min, in order to visualize the nuclei. Then, cells were washed three times with PBS and mounted on slices using Aqua-Poly/Mount coverslipping medium (Polysciences, Inc. Eppelheim, Germany). For immunofluorescence, cells were permeabilized with 0.2% Triton X-100 in PBS for 15 min. Then, cells were washed three times with PBS and blocked one hour with 10% fetal bovine serum, 5% nonfat dried milk, and 0.1% Triton X-100 in PBS, for anti-HA antibody, or with 3% BSA in PBS for glycogen synthase antibody. Cells were then incubated overnight at 4ºC with 1/200 dilution of anti-HA (Sigma-Aldrich, Madrid, Spain) or anti-GS (rabbit monoclonal antibody against the C-term of muscular glycogen synthase; Epitomics/AntibodyBcn, Barcelona, Spain) in blocking solution. Samples were washed three times with PBS and incubated with a 1/500 dilution of anti-mouse Alexa-Fluor 633 or anti-rabbit Alexa-Fluor 633 (Invitrogen, Madrid, Spain), respectively. Finally, samples were processed as described above for direct fluorescence. For R6 subcellular localization, images were acquired with a upright Leica DM RXA2 microscope and for co-localization assays with a Leica TCS SL confocal microscope (Leica, Wetzlar, Germany) using an PL APO 63x oil 1.4 N.A. immersion objective. Images were treated with the ImageJ 1.43c software (Wayne Ras-band, National Institutes of Health, Bethesda, MD).

2.8 FRET experiments. Fluorescence Resonance Energy Transfer (FRET) measurements were performed using the acceptor photobleaching approach (Karpova et al. , 2003). Cyan and yellow fluorescence protein (CFP and EYFP) were used as the respective donor and acceptor FRET pair. A 458 nm excitation laser line and a 465-510 nm band width for emission for CFP and a 514 nm excitation laser line and a 525-650 nm band width for emission for EYFP were used as donor and acceptor channels. Neuro-2a cells were transfected with either pEYFP-R6 (acceptor) + pCFP-laforin (donor) or pEYFP (empty) + pCFP-laforin plasmids. FRET efficiency was accomplished by comparing the donor's fluorescence intensity in the cells transfected with both

donor and acceptor fluorescent proteins before (prebleached) and after (postbleached) depleting the acceptor fluorescence at least 60% of the initial fluorescence by photobleaching. FRET efficiency values were obtained using the following equation: FRETeff(%)= [(Donor $_{postbleached}$ − Donor $_{prebleached}$) / Donor $_{postbleached}$) x100]. Images (8 bits, 512 x 512 pixels, two airy pinhole units and 2.7 x zoom) were taken in a Leica TCS SL confocal microscope with a PL APO 63x 1.4 N.A. oil objective using the Leica Confocal Software (Leica, Wetzlar, Germany). If FRET is present, the fluorescence intensity of donor should increase after acceptor is photobleached.

2.9 Statistical data analysis. Data are expressed as means with standard deviation. Statistical significance of differences between the groups was evaluated by a paired Student's t-test with two-tailed distribution. The significance has been considered at * $p < 0.05$, ** $p < 0.01$, *** $p < 0.001$, as indicated in each case.

3. RESULTS
3.1. Laforin interacts with the PP1 glycogenic regulatory subunit R6
In order to study a possible relationship between the PP1 glycogen targeting subunit R6 (PPP1R3D) and laforin or/and malin, we performed yeast-two hybrid assays. As shown in Figure 1 (left panel), we detected a solid two-hybrid interaction between R6 and laforin but not with malin, even though both proteins were expressed at the same level (Fig.1, right panel). There was no difference in the strength of interaction when using different protein fusions (LexA or GAD), confirming the positive interaction between R6 and laforin. Since laforin and malin form a functional complex, we carried out also yeast triple-hybrid assays overexpressing in addition either malin or laforin, but this strategy did not improve the interaction between the corresponding partners (data not shown).

To validate the interaction between R6 and laforin in mammalian cells we performed a co-immunoprecipitation approach. We overexpressed in a murine neuroblastoma cell line, Neuro-2a (N2a), a myc-tagged R6 plasmid and laforin labeled with HA. Myc-R6 was immunoprecipitated using an anti-myc antibody, and HA-laforin appeared in the co-immunoprecipitates but only when R6 was present (Fig. 2A), indicating that R6 is able to interact with laforin in mammalian cells.

We took advantage of fluorescent resonance energy transfer (FRET) technology to confirm the interaction between R6 and laforin. We constructed a R6 fusion protein with yellow fluorescent protein (EYFP) attached on its N-terminus as a FRET acceptor. As a donor we used a cyan fluorescent protein (CFP) fused to the N-terminus of laforin. When both constructs were co-expressed in N2a cells, a FRET signal was observed which was significantly higher than the one present in cells expressing EYFP alone and CFP-laforin (Fig. 2B), indicating that laforin and R6 are close enough to enable energy transfer. All these results indicate a physical interaction between laforin and R6.

3.2. The laforin-malin complex is able to ubiquitinate R6
Malin is a RING-type E3-ubiquitin ligase able to ubiquitinate itself and its partner protein laforin, as well as other proteins related to energy metabolism, such as

AMPK or other PP1 regulatory subunits like R5/PTG [(Solaz-Fuster, Gimeno-Alcaniz, 2008), (Moreno et al. , 2010)]. It has been reported that laforin may recruit specific substrates to be ubiquitinated by malin. Thus, laforin and malin act as a functional complex regulating the ubiquitination of many substrates. As we have observed the interaction of R6 with laforin, we decided to analyze if laforin could recognize R6 as a putative malin substrate. With this aim, we performed an ubiquitination assay in HEK-293 cells using a 6xHis tagged ubiquitin. Cells were lysed in denaturing buffer containing the chaotropic agent guanidinium hydrochloride to prevent the action of deubiquitinating enzymes (Kaiser and Tagwerker, 2005). To detect R6-ubiquitinated forms, we purified the ubiquitinated proteins by metal-affinity chromatography. Then, we analyzed the affinity-purified ubiquitin conjugates by SDS-PAGE and Western blot analysis using specific antibodies against the protein of interest (Fig. 3). We noted a discrete pattern of R6 ubiquitination due to the presence of both malin and laforin proteins (Fig. 3, lane 4). Although at lower intensity, ubiquitinated forms of R6 were also present if only malin was overexpressed, probably due to the presence of endogenous laforin in HEK-293 cells (Fig. 3, lane 3). No major ubiquitinated forms were detected when only laforin was overexpressed (Fig. 3, lane 2) or in the absence of overexpressed laforin and malin (Fig. 3, lane 1). These data indicate that a functional laforin-malin complex is needed to carry out R6 ubiquitination, supporting our previous results indicating that laforin assists in malin-directed ubiquitination.

To evaluate the specificity of malin-dependent R6 ubiquitination, we tested if another RING-type E3 ubiquitin ligase could ubiquitinate R6. With this purpose, we overexpressed R6 in combination with Mdm2, a known p53 ubiquitin ligase. In this case, no ubiquitinated bands of R6 appeared (Fig. 3C), verifying the specificity of this posttranslational modification. Notably, the malin-dependent ubiquitination pattern of R6 is different from the one from R5/PTG, a known substrate of the laforin-malin complex [(Solaz-Fuster, Gimeno-Alcaniz, 2008), (Worby, Gentry, 2008)]. While R6 ubiquitination pattern presents a major predominant band, corresponding probably to the incorporation of two ubiquitin moieties, in R5/PTG predominates the presence of ubiquitinated conjugates of high molecular weight (Fig.3B, compare lanes 4 and 6).

It has been reported that the laforin-malin complex induces the polyubiquitination of R5/PTG and AMPK β-subunits via Lys63-linked ubiquitin chains (Moreno, Towler, 2010). In order to elucidate the topology of the ubiquitin chains present on R6, we overexpressed 6xHis-ubiquitin mutants in which residues lysine 48 or 63 were replaced by arginine. To improve the accumulation of ubiquitinated proteins we used the proteasomal inhibitor MG132. As we can observe in Fig. 4, when the K48R ubiquitin mutant was used, R6-ubiquitinated levels were similar to wild type (lanes 5 and 6 in comparison to lanes 3 and 4), indicating that the residue K48 of ubiquitin is not essential in the process. On the contrary, when the K63 residue was mutated to arginine, the formation of high molecular weight ubiquitin conjugates was prevented, demonstrating the importance of this residue in the ubiquitin chain formation (Fig. 4, lane 7 and 8). However, this mutant did not prevent the formation of R6-ubiquitinated species containing only one ubiquitin moiety (Fig. 4, lanes 7 and 8).

To ascertain the topology of ubiquitin linkages incorporated by malin on R6, we performed an ubiquitination assay employing a lysine-less ubiquitin

(KO), which has all the seven lysine residues mutated by arginine and hence, it cannot form ubiquitin chains (Fig. 4, lanes 9 and 10). As expected, this KO-ubiquitin mutant prevented the formation of high molecular weight polyubiquitin chains (Fig. 4, lanes 9 and 10). However, a predominant band remained at the molecular weight corresponding to +1 ubiquitin attached to R6. These results support the data presented above with the K63R mutant, where only a similar major band was detected (Fig. 4, lane 7 and 8). These findings indicate that malin promotes the incorporation of a single ubiquitin moiety in one site on R6. Thus, R6 is the first substrate of the laforin-malin complex which is mono-ubiquitinated. When using the KO-ubiquitin form we also detected a band corresponding to +2 ubiquitins (Fig. 4, lanes 9 and 10), which was also present when wild type ubiquitin was present in the assay (Fig. 4, lanes 3 and 4). Curiously, this band is the main form when using Flag-R6 as substrate (Fig. 3, lane 4). The difference in the ubiquitination pattern between the experiments described in Fig. 3 and 4 could be due to different accessibility of the laforin-malin complex to the distinct tagged-R6 forms. Taking all these results together, we suggest that the laforin-malin complex, in addition to its recognized role attaching K63-linked ubiquitin chains on its corresponding substrate, may also produce the mono/multi-ubiquitination of the substrate, as in the case of R6.

3.3. R6 glycogenic activity is impaired by the laforin-malin complex in N2a cells

Next, we tested the possible effect of the laforin-malin complex on the glycogenic activity of R6. First of all, we measured the increase in glycogen levels as a consequence of R6 overexpression in N2a cells. When these cells were transfected with an empty vector, the levels of glycogen were almost undetectable, suggesting an auto-inactivated state of the glycogenic machinery (Vilchez, Ros, 2007). On the contrary, when R6 was overexpressed, glycogen levels were detected at high levels. This effect was dose-dependent on the amount of R6 present, indicating that the glycogenic activity was dependent on the expression of R6 (Fig. 5A). The glycogenic activity of R6 was due to an activation of endogenous glycogen synthase activity in these cells, demonstrated by the appearance of faster mobility dephosphorylated bands, as suggested by western blotting analysis (Fig. 5B, left panel). We could not detect an effect of R6 on the phosphorylation status of endogenous phosphorylase, probably due to the low amount of this enzyme present in N2a cells. However, we detected a robust interaction between R6 and phosphorylase by yeast two-hybrid analysis (Fig. 5B, right panel), indicating that an effect of R6 on endogenous phosphorylase is likely to occur.

Then, we co-transfected N2a cells with plasmids expressing R6, malin and laforin. This led to a down-regulation of both glycogen and R6 protein levels (Fig. 5C), reaching a 50% decrease of glycogen production when laforin and malin were present. These data were in agreement with a reported downregulation of the glycogenic activity of R6 by the laforin-malin complex in CHO-IR cells (Worby, Gentry, 2008). Therefore, the laforin-malin complex is able to downregulate R6 protein levels, leading to a decrease in its glycogenic activity.

3.4. Laforin-malin dependent ubiquitination of R6 leads to its lysosomal degradation

To analyze whether the laforin-malin dependent ubiquitination of R6 could mark it for proteasomal degradation, we decided to inhibit proteasome activity and check whether this prevented the downregulation of R6 protein levels by the laforin-malin complex. With this purpose, we transfected HEK-293 cells with plasmids expressing only R6, or R6, laforin and malin. Then, cells were treated with the proteasomal inhibitor lactacystin. In cells expressing only R6, no differences were observed on the steady-state protein levels of R6 when using lactacystin in comparison to untreated cells (Fig. 6A, compare lane 1 and 3). Cells co-expressing R6 and the laforin-malin complex presented lower levels of R6 protein (Fig. 6A, lane 4), and these levels did not increase in cells treated with lactacystin (Fig. 6A, lane 6). All these results demonstrate that the laforin-malin induced downregulation of R6 occurs by a proteasome-independent manner.

Subsequently, we tested whether the laforin-malin dependent ubiquitination of R6 acts as a signal for lysosomal degradation. In this regard, we treated HEK-293 cells with ammonium chloride and leupeptin, two compounds that impair lysosomal function. In cells expressing only R6, the action of the lysosomal inhibitors produced an accumulation of the steady-state levels of the R6 protein (Fig. 6A, lane 2; Fig. 6B), suggesting an involvement of the autophagic pathway in the regular degradation of R6. In cells co-expressing R6 and the laforin-malin complex, the treatment with the lysosomal inhibitors produced the accumulation of higher levels of the R6 protein (Fig. 6A, lane 5; Fig. 6B) in comparison to untreated cells. These data suggest that the downregulation of R6 protein occurs mainly through the lysosomal pathway. These results are in agreement with the evidence reported above that R6 was mono/multiubiquitinated and, when polyubiquitinated, it was by K63-linked ubiquitin chains (Fig. 4), which are recognized signals for autophagic degradation.

3.5. R6, laforin and malin co-localize with endogenous glycogen synthase in N2a cells

Finally, we also studied the subcellular localization of R6, laforin and malin in N2a cells. To this end, we transfected N2a cells with the same EYFP-R6 and CFP-laforin tagged plasmids used for the FRET analysis (see above; Fig. 2B). We also co-transfected the cells with a HA-tagged malin construct and performed an immunocytochemical detection using appropriated antibodies. As it is shown in Figure 7A, we detected R6 in structures occupying almost all the cytoplasm of the N2a cells, although occasionally, R6 presented a patched-pattern as well (data not shown). In these structures, we were also able to detect the presence of laforin and malin, evidencing a co-localization of the three proteins in these subcellular localizations (Fig 7B). As R6 has glycogenic activity and has a carbohydrate binding module on its structure, we checked whether other components of the glycogenic machinery co-localized with R6. With this aim, we used a specific antibody in order to detect endogenous glycogen synthase (GS), one of the main components of the glycogenic machinery. We found that glycogen synthase co-localized in structures where R6 and laforin were also present (Fig. 7C). All these results suggest that the four proteins, R6, laforin, malin and GS are localized in the same structures, possibly sites of glycogen synthesis, revealing a common role of these proteins on the regulation of glycogen homeostasis in N2a cells. Binding of malin to

these structures does not depend on the presence of laforin, since after silencing laforin expression, malin still co-localized with R6 and glycogen synthase (Supplementary Fig. S1), probably because of its capacity to interact directly with components of the glycogenic machinery (glycogen synthase, neuronatin) [(Lohi et al. , 2005), (Sharma et al. , 2011)].

4. DISCUSSION

Lafora disease (LD, OMIM 254780) is a fatal progressive myoclonus epilepsy characterized by epilepsy, neurodegeneration and accumulation of polyglucosan inclusions (Lafora bodies) in the brain and other peripheral tissues [(Gentry et al. , 2012), (Roma-Mateo et al. , 2012)]. Since one of the hallmarks of the disease is the accumulation of insoluble poorly-branched forms of glycogen, it has been suggested that LD is related to other diseases in which glycogen homeostasis is disturbed. The study of the molecular basis of LD has provided new concepts to understand the regulation of glycogen formation. For example, it has been reported that glycogen synthase, in addition to adding new glucose molecules to the glycogen chain, it also incorporates by error glucose moieties that are phosphorylated (Tagliabracci et al. , 2011). The presence of phosphate in the glycogen molecule impairs the formation of regular branched chains, resulting in a poorly-branched phosphorylated insoluble polyglucosan. One of the genes related to LD (EPM2A) encodes laforin, a glucan phosphatase involved in the dephosphorylation of glycogen. In the absence of laforin, glycogen remains phosphorylated leading to the formation of Lafora bodies (Gentry, Roma-Mateo, 2012). In addition, laforin interacts with the product of the second gene related to LD (EPM2B), named malin, an E3-ubiquitin ligase of the RING type [(Gentry et al. , 2005), (Lohi et al. , 2005)]. Laforin and malin form a functional complex in which laforin recruits specific substrates to be ubiquitinated by malin.

One of the first characterized substrates of the laforin-malin complex was R5/PTG (PPP1R3C), a glycogen targeting subunit of protein phosphatase PP1. Results from different groups have demonstrated that in cellular models, the laforin-malin complex ubiquitinates R5/PTG, decreases R5/PTG protein levels and downregulates its glycogenic activity [(Vilchez, Ros, 2007), (Solaz-Fuster, Gimeno-Alcaniz, 2008), (Worby, Gentry, 2008)]. It has also been reported that the laforin-malin complex also downregulates the activity of glycogen synthase (GS) (Vilchez, Ros, 2007), glycogen debranching enzyme (GDE/AGL) (Cheng et al. , 2007) and neuronatin, a small protein that stimulates glycogenesis (Sharma et al. , 2011). All these results point to a major role of the laforin-malin complex in the regulation of glycogen biosynthesis. The action of the laforin-malin complex becomes crucial in the neurons, since in the absence of a functional laforin-malin complex, these cells start to accumulate poorly branched polyglucosans (Lafora bodies). In regular conditions, neurons do not accumulate glycogen since they have all the glycogenic machinery in the inactivated state (Vilchez, Ros, 2007). However, the expression of R5/PTG in these cells induces glycogen synthesis (Vilchez, Ros, 2007) and defects in the laforin-malin complex also induce the formation of polyglucosan bodies. The relationship between the laforin-malin complex and R5/PTG became evident when it was demonstrated that mice with deficiencies in both laforin and R5/PTG did not accumulate polyglucosan bodies (Turnbull et al. , 2011).

In this work we have extended the analysis of the functionality of the laforin-malin complex on glycogen biosynthesis to an additional PP1 targeting subunit present in brain, namely PPP1R3D or R6. This is a glycogen binding protein of 33 kDa widely distributed in a variety of tissues (Armstrong, Browne, 1997). This glycogenic subunit is particularly interesting since we have recently described that, in pancreatic beta cells, it participates in the regulation of the phosphorylation status and activity of the catalytic subunit of the AMPK complex, a key cellular metabolic sensor (Garcia-Haro, Garcia-Gimeno, 2010), and this role is not shared by other PP1 glycogenic targeting subunits such as R5/PTG or GL. We demonstrate in this work that R6 interacts with laforin and that it becomes ubiquitinated by malin. In this way, R6 follows a similar way of regulation as R5/PTG (see above). However, we have noticed that the ubiquitination of R6 targets it for autophagic degradation. The fact that the reduction of R6 protein levels induced by the co-expression of laforin and malin is prevented by the presence of lysosome inhibitors (ammonium chloride and leupeptine) but not by the presence of a proteasome inhibitor (lactacystin) supports this notion. In addition, we present evidence indicating that the laforin-malin complex mono/multiubiquitinates R6 and additionally introduces K63-linked polyubiquitin chains, which are determinants described as signals for autophagic degradation.

5. CONCLUSIONS

Our results indicate that the laforin-malin complex plays a crucial role in regulating glycogen biosynthesis in neurons. This complex downregulates the function of different PP1 targeting subunits [R5/PTG, R6 (this work)], ensuring the maintenance of glycogen synthase in its phosphorylated inactive state, preventing in this way glycogen biosynthesis. In the absence of a functional laforin-malin complex, the glycogenic activity of R5/PTG and R6 increases, leading to the accumulation of poorly-branched glycogen in cells that do not normally accumulate these deposits, what might trigger the death of the neurons.

7. REFERENCE LIST

Armstrong CG, Browne GJ, Cohen P, Cohen PT. PPP1R6, a novel member of the family of glycogen-targetting subunits of protein phosphatase 1. FEBS Lett. 1997;418:210-4.

Bollen M, Peti W, Ragusa MJ, Beullens M. The extended PP1 toolkit: designed to create specificity. Trends Biochem Sci. 2010;35:450-8.

Chan TM, Exton JH. A rapid method for the determination of glycogen content and radioactivity in small quantities of tissue or isolated hepatocytes. Anal. Biochem. 1976;71:96-105.

Cheng A, Zhang M, Gentry MS, Worby CA, Dixon JE, Saltiel AR. A role for AGL ubiquitination in the glycogen storage disorders of Lafora and Cori's disease. Genes Dev. 2007;21:2399-409.

Esteves SL, Domingues SC, da Cruz e Silva OA, Fardilha M, da Cruz e Silva EF. Protein phosphatase 1alpha interacting proteins in the human brain. OMICS. 2012;16:3-17.

Garcia-Haro L, Garcia-Gimeno MA, Neumann D, Beullens M, Bollen M, Sanz P. The PP1-R6 protein phosphatase holoenzyme is involved in the glucose-induced dephosphorylation and inactivation of AMP-activated protein kinase, a key regulator of insulin secretion, in MIN6 beta cells. Faseb J. 2010;24:5080-91.

Gentry MS, Roma-Mateo C, Sanz P. Laforin, a protein with many faces: glucan phosphatase, adapter protein, and others. The FEBS journal. 2012:doi: 10.1111/j.742-4658.2012.08549.x.

Gentry MS, Worby CA, Dixon JE. Insights into Lafora disease: malin is an E3 ubiquitin ligase that ubiquitinates and promotes the degradation of laforin. Proc Natl Acad Sci U S A. 2005;102:8501-6.

Heroes E, Lesage B, Gornemann J, Beullens M, Van Meervelt L, Bollen M. The PP1 binding code: a molecular-lego strategy that governs specificity. The FEBS journal. 2012:doi: 10.1111/j.742-4658.2012.08547.x.

Kaiser P, Tagwerker C. Is this protein ubiquitinated? Methods in enzymology. 2005;399:243-8.

Karpova TS, Baumann CT, He L, Wu X, Grammer A, Lipsky P, et al. Fluorescence resonance energy transfer from cyan to yellow fluorescent protein detected by acceptor photobleaching using confocal microscopy and a single laser. J Microsc. 2003;209:56-70.

Li M, Brooks CL, Wu-Baer F, Chen D, Baer R, Gu W. Mono- versus polyubiquitination: differential control of p53 fate by Mdm2. Science. 2003;302:1972-5.

Lohi H, Ianzano L, Zhao XC, Chan EM, Turnbull J, Scherer SW, et al. Novel glycogen synthase kinase 3 and ubiquitination pathways in progressive myoclonus epilepsy. Hum Mol Genet. 2005;14:2727-36.

Ludin K, Jiang R, Carlson M. Glucose-regulated interaction of a regulatory subunit of protein phosphatase 1 with the Snf1 protein kinase in Saccharomyces cerevisiae. Proc Natl Acad Sci U S A. 1998;95:6245-50.

Moreno D, Towler MC, Hardie DG, Knecht E, Sanz P. The laforin-malin complex, involved in Lafora disease, promotes the incorporation of K63-linked ubiquitin chains into AMP-activated protein kinase beta subunits. Mol. Biol. Cell. 2010;21:2578-88.

Paumi CM, Menendez J, Arnoldo A, Engels K, Iyer KR, Thaminy S, et al. Mapping protein-protein interactions for the yeast ABC transporter Ycf1p by

integrated split-ubiquitin membrane yeast two-hybrid analysis. Mol Cell. 2007;26:15-25.

Roach PJ, Depaoli-Roach AA, Hurley TD, Tagliabracci VS. Glycogen and its metabolism: some new developments and old themes. Biochem J. 2012;441:763-87.

Roma-Mateo C, Sanz P, Gentry MS. Deciphering the role of malin in the lafora progressive myoclonus epilepsy. IUBMB Life. 2012;64:801-8.

Sharma J, Rao SN, Shankar SK, Satishchandra P, Jana NR. Lafora disease ubiquitin ligase malin promotes proteasomal degradation of neuronatin and regulates glycogen synthesis. Neurobiol. Dis. 2011;44:133-41.

Solaz-Fuster MC, Gimeno-Alcaniz JV, Ros S, Fernandez-Sanchez ME, Garcia-Fojeda B, Criado Garcia O, et al. Regulation of glycogen synthesis by the laforin-malin complex is modulated by the AMP-activated protein kinase pathway. Hum Mol Genet. 2008;17:667-78.

Tagliabracci VS, Heiss C, Karthik C, Contreras CJ, Glushka J, Ishihara M, et al. Phosphate incorporation during glycogen synthesis and Lafora disease. Cell Metab. 2011;13:274-82.

Turnbull J, DePaoli-Roach AA, Zhao X, Cortez MA, Pencea N, Tiberia E, et al. PTG depletion removes Lafora bodies and rescues the fatal epilepsy of Lafora disease. PLoS genetics. 2011;7:e1002037.

Vernia S, Solaz-Fuster MC, Gimeno-Alcaniz JV, Rubio T, Garcia-Haro L, Foretz M, et al. AMP-activated protein kinase phosphorylates R5/PTG, the glycogen targeting subunit of the R5/PTG-protein phosphatase 1 holoenzyme, and accelerates its down-regulation by the laforin-malin complex. J Biol Chem. 2009;284:8247-55.

Vilchez D, Ros S, Cifuentes D, Pujadas L, Valles J, Garcia-Fojeda B, et al. Mechanism suppressing glycogen synthesis in neurons and its demise in progressive myoclonus epilepsy. Nature Neurosci. 2007;10:1407-13.

Worby CA, Gentry MS, Dixon JE. Malin decreases glycogen accumulation by promoting the degradation of protein targeting to glycogen (PTG). J Biol Chem. 2008;283:4069-76.

FIGURE LEGENDS

Figure 1: R6 interacts with laforin by yeast two-hybrid analysis. Left panel: yeast THY-AP4 strain was transformed with plasmids pBTM-R6 (LexA-R6) and pACT2 (GAD), pACT2-malin (GAD-malin) or pACT2-laforin (GAD-laforin), or with plasmid pGADT7-R6 (GAD-R6) and plasmids pBTM (LexA), pBTM-malin (LexA-malin) and pEG202-laforin (LexA-laforin). Protein interaction was estimated using the yeast two-hybrid system, by measuring the β-galactosidase activity. Values correspond to means from at least 6 different transformants (± SD, standard deviation). Right panel, protein expression analyzed by Western blotting using anti-HA antibodies (for the GAD-fusions) and anti-LexA (for the LexA-fusions) of three independent transformants.

Figure 2: R6 interacts with laforin in mammalian N2a cells. A) Laforin co-immunoprecipitates with R6. Protein extracts were prepared from N2a cells transfected with pCMV-HA-laforin and pCMV-myc-R6. One μL of anti-myc antibody was used to immunoprecipitate the extracts, followed by immunoblot analysis with anti-HA (upper panel) and anti-myc (lower panel) antibodies (IP). Crude extracts (CE, 20 μg) were also analyzed by immunoblotting with the indicated antibodies. B) FRET analysis. N2a cells transfected with CFP-laforin and EYFP-R6 were fixed using paraformaldehyde followed by FRET analysis using FRET photobleaching technique as described in Material & Methods. On the left, EYFP-R6 was used as a FRET acceptor (upper panels) and CFP-laforin as FRET donor (lower panels). The area analyzed is indicated as ROI (region of interest). Pre: before and Post: after depleting the acceptor fluorescence by photobleaching. On the right, FRET efficiency values correspond to means from 15 to 30 different cells (bars indicate ± SD, standard deviation), ***$p < 0.001$. The same analysis was performed using EYFP as acceptor control.

Figure 3: The laforin-malin complex is able to ubiquitinate R6. A) HEK-293 cells were transfected with the indicated vectors. Cells were then lysed and ubiquitinated proteins purified by metal-affinity chromatography. Bound material (Bound) as well as the clarified extract (CE, 50 μg) was analyzed by SDS-PAGE and immunoblotting using anti-Flag antibodies. Clarified extract was also analyzed using anti-HA antibodies. (+1Ub, +2Ub, indicates the position of R6 derivatives containing one or two ubiquitin moieties). B) HEK-293 cells were transfected with pCMV(empty plasmid) or pCMV-myc-R5 and the indicated combination of plasmids. Cell extracts were analyzed as described above, but using anti-myc antibodies. C) HEK-293 cells transfected with pCMV-Mdm2 and the indicated combination of plasmids were analyzed as described in part A). Clarified extract was also analyzed with anti-Mdm2 antibodies.
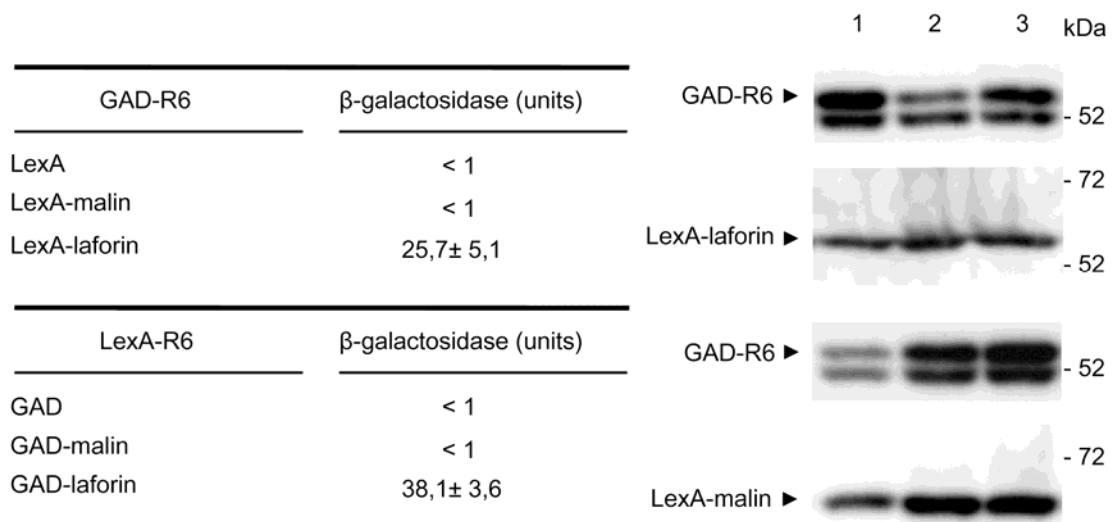
Figure 4: The laforin-malin complex promotes mono/multi- and polyubiquitination of R6. HEK-293 cells were transfected with the indicated vectors and twenty-four hours after transfection treated with 25 μM MG132 for 6 hours. Then, ubiquitinated proteins were purified by metal-affinity chromatography. Clarified extracts (CE, 50 μg) and bound material (Bound) were analyzed by immunoblotting using anti-myc antibodies. Clarified extracts were also analyzed with anti-HA antibodies.
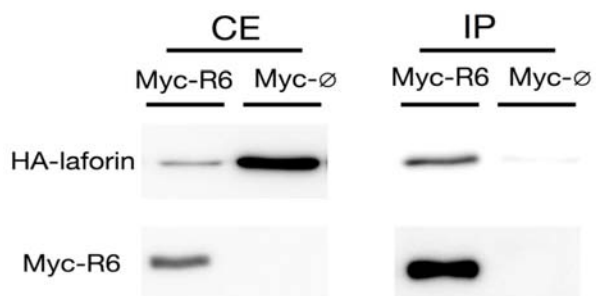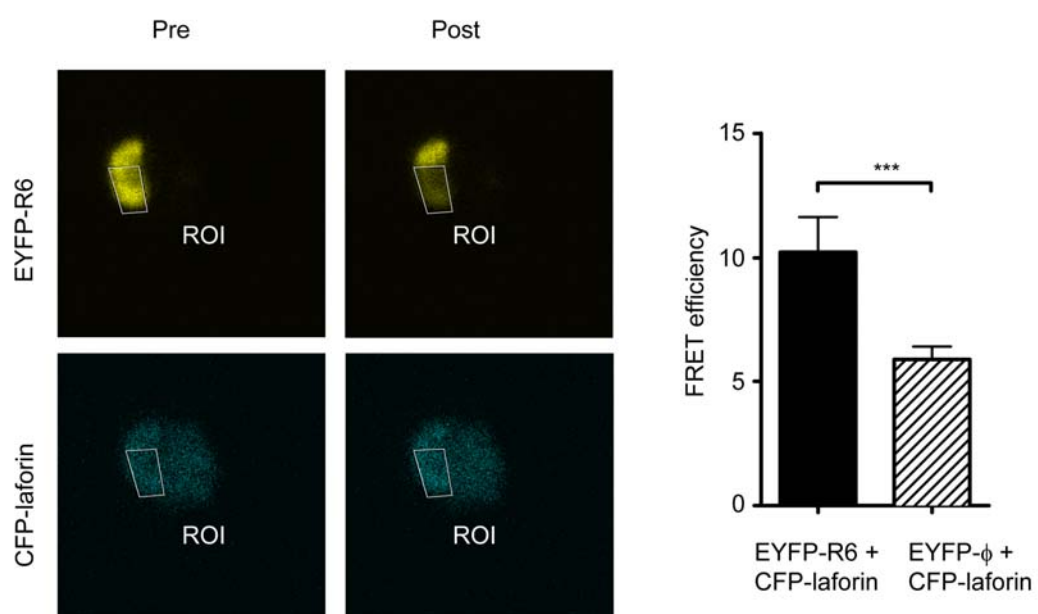
Figure 5: The laforin-malin complex modulates R6 glycogenic activity. A) R6 glycogenic activity in N2a cells is dose-dependent. N2a cells were transfected using 1 µg (R6) or 1/3 µg (R6/3) of pFlag-R6 plasmid. Forty-eight hours after transfection, the amount of glycogen was determined as described in Material and Methods. On the right panel, a representative Western blot analysis (using anti-Flag) of protein expression in the cell extracts (20 µg) used for the glycogen determination is shown. The same extracts were analyzed with anti-tubulin as loading control. B) Effect of R6 on glycogen biosynthesis enzymes. Left panel, N2a cells were transfected using 1 µg of pFlag-R6 or empty plasmid. Twenty-four hours after transfection, cell extracts (20 µg) were analyzed by western blotting using the corresponding antibodies: anti-glycogen synthase (notice the faster migrating bands corresponding to dephosphorylated forms of GS), anti-phosphoSer641 glycogen synthase and anti-Flag antibodies. Tubulin was also detected and used as loading control. Right panel, a yeast two-hybrid analysis of R6 and glycogen phosphorylase. Yeast THY-AP4 strain was transformed with plasmids pEG202-Phosphorylase (LexA-Ph) and pGADT7-R6 (GAD-R6), or the corresponding empty plasmids. Protein interaction was estimated using the yeast two-hybrid system, by measuring the β-galactosidase activity. Values correspond to means from at least 6 different transformants (± SD, standard deviation). C) The laforin-malin complex downregulates R6 glycogenic activity. Left panel, N2a cells were transfected with pFlag (empty vector), pFlag-R6 (R6) or pFlag-R6 with pCMV-HA-laforin and pcDNA3-HA-malin (R6 + Laf/Mal). Forty-eight hours after transfection, the amount of glycogen was determined as described in Material and Methods. Glycogen content was expressed as a percentage of the amount of glycogen present when pFlag-R6 was expressed. Bars indicate standard deviation of three independent experiments (**p < 0.01). Right panel, a representative Western blot analysis (using anti-Flag and anti-HA) of protein expression in the cell extracts (20 µg) used for the glycogen determination is shown. The same extracts were analyzed with anti-tubulin as loading control.
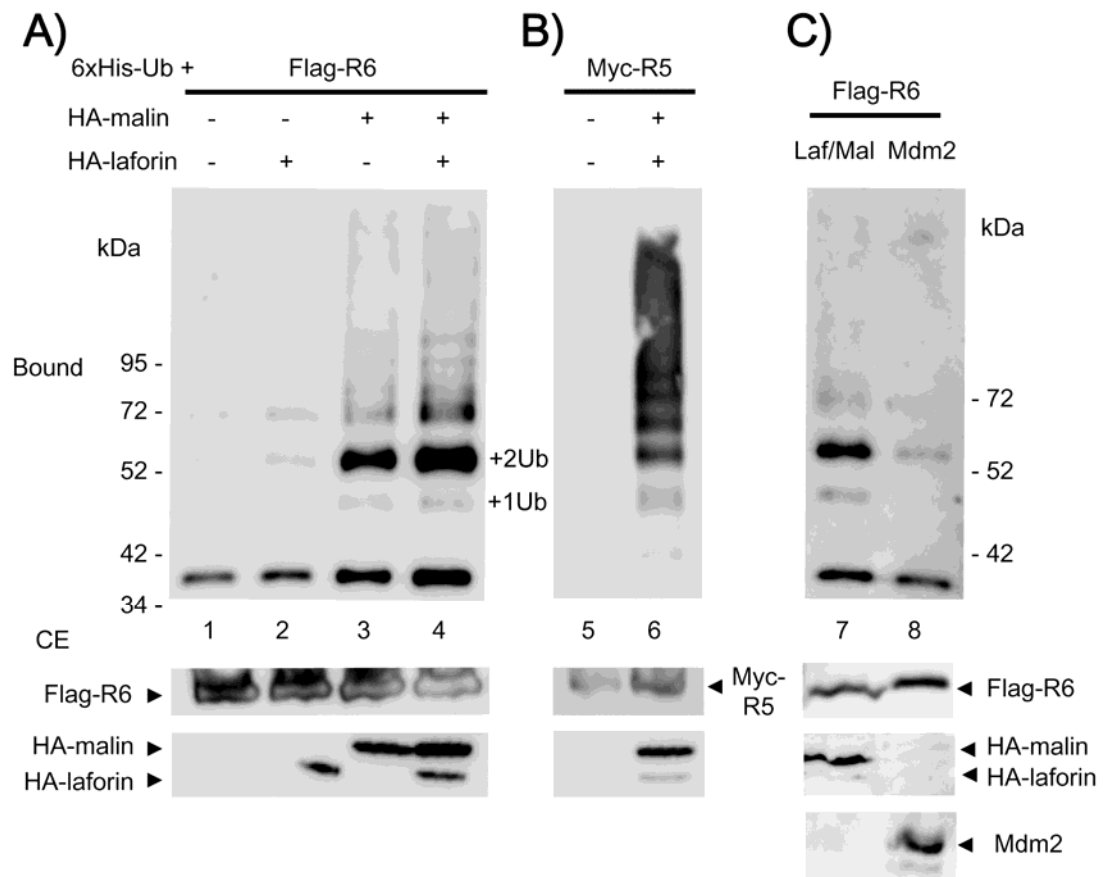
Figure 6: R6 ubiquitination acts as a signal for autophagic degradation. A) HEK-293 cells were transfected with the indicated vectors. Eighteen hours after transfection, cells were treated with ammonium chloride (20 mM)/ leupeptin (100 µM) or lactacystin (5 µM) for 6 hours. Then, cells were lysed and the extracts (20µg) were analyzed by immunoblotting using the indicated antibodies (anti-myc, anti-HA and anti-tubulin). B) The intensity of the bands related to the levels of tubulin is plotted (mean of four different experiments). Bars indicate standard deviation; *p < 0.05; **p < 0.01.
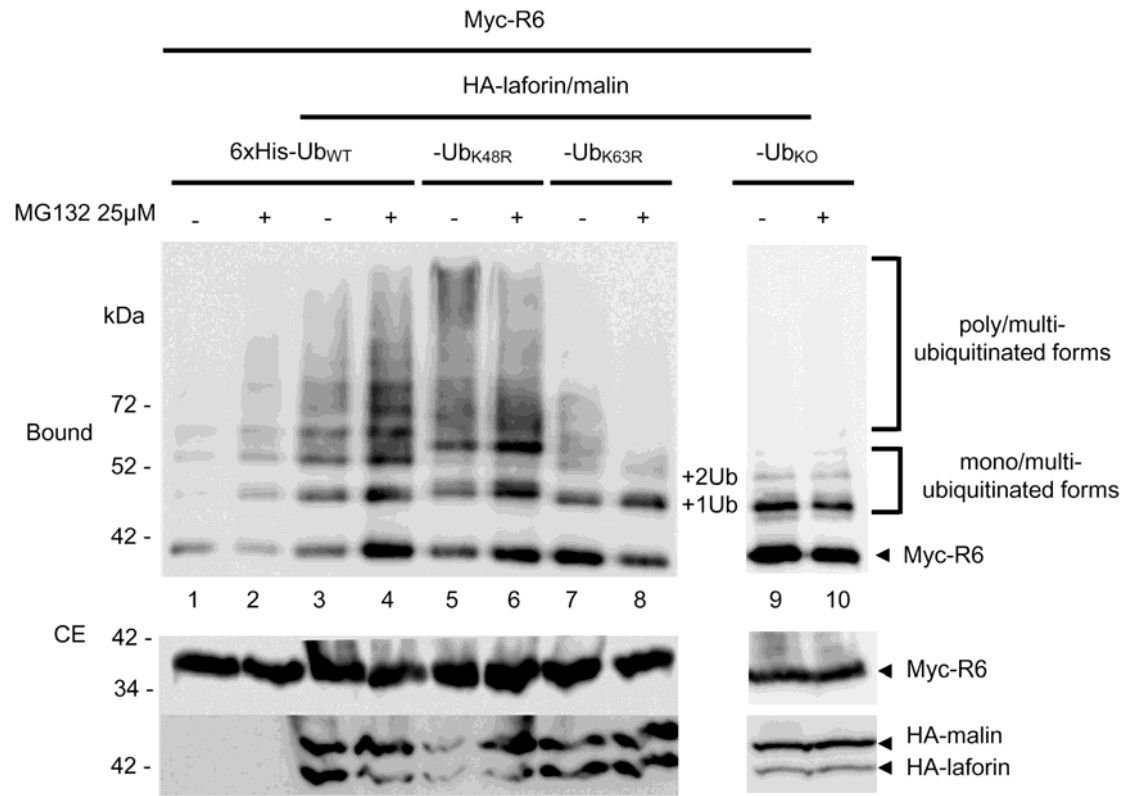
Figure 7: Co-localization of R6, laforin, malin and glycogen synthase in N2a cells. A) N2a cells were transfected with pEYFP-R6 plasmid and treated with DAPI to stain the nucleus. The subcellular localization of EYFP-R6 was carried out as described in Material and Methods. The three images were subjected to merge analysis. B) N2a cells were co-transfected with pEYFP-R6, pCFP-laforin and pcDNA3-HA-malin. The subcellular localization of EYFP-R6, CFP-laforin and HA-malin was carried out as described in Material and Methods. Images were obtained by using confocal microscopy as described in Material and Methods and magnified x2.5 as indicated (bars indicate 20 μm). The three images were subjected to merge analysis. C) N2a cells were transfected with
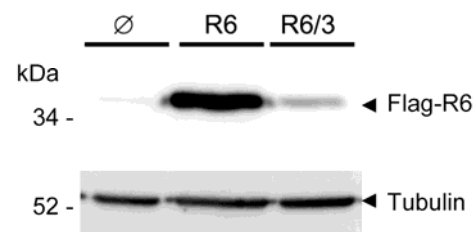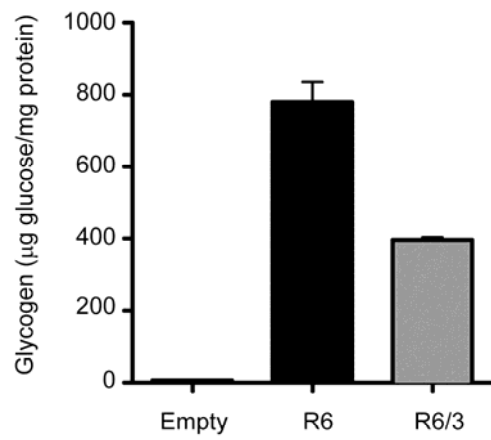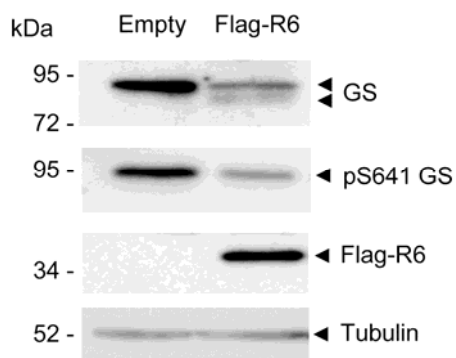
plasmids as indicated in B). The subcellular localization of EYFP-R6, CFP-laforin and endogenous glycogen synthase was carried out as indicated in Materials and Methods (anti-glycogen synthase was used as primary antibody and Alexa-Flour 633 as secondary antibody). Confocal images were magnified as indicated (bars indicate 10 μm) and subjected to merge analysis.

GAD-R6	β-galactosidase (units)
LexA	< 1
LexA-malin	< 1
LexA-laforin	25,7± 5,1

LexA-R6	β-galactosidase (units)
GAD	< 1
GAD-malin	< 1
GAD-laforin	38,1± 3,6

A)

	CE		IP	
	Myc-R6	Myc-∅	Myc-R6	Myc-∅

HA-laforin

Myc-R6

B)

A)

6xHis-Ub +	Flag-R6			
HA-malin	-	-	+	+
HA-laforin	-	+	-	+

Bound

kDa

95 -

72 -

52 - → +2Ub

→ +1Ub

42 -

34 -

1   2   3   4

CE

Flag-R6 ►

HA-malin ►
HA-laforin ►

B)

Myc-R5

	-	+

5   6

◄ Myc-R5

C)

Flag-R6

Laf/Mal   Mdm2

kDa

- 72

- 52

- 42

7   8

◄ Flag-R6

◄ HA-malin
◄ HA-laforin

◄ Mdm2

Myc-R6

HA-laforin/malin

| 6xHis-Ub$_{WT}$ | | | | -Ub$_{K48R}$ | | -Ub$_{K63R}$ | | -Ub$_{KO}$ | |

MG132 25µM   -   +   -   +   -   +   -   +   -   +

Bound

kDa

72 -

52 -

42 -

poly/multi-
ubiquitinated forms

+2Ub
+1Ub

mono/multi-
ubiquitinated forms

◄ Myc-R6

1   2   3   4   5   6   7   8   9   10

CE   42 -

34 -

42 -

◄ Myc-R6

◄ HA-malin
◄ HA-laforin

A)

B)

LexA-Ph	β-galactosidase (units)
GAD	< 1
GAD-R6	154 ± 24

C)

A)

B)

A)

DAPI

EYFP-R6

Merge

B)

20µ

x2,5

EYFP-R6

CFP-laforin

HA-malin

Merge

C)

EYFP-R6

CFP-laforin

10µm

10µm

Glycogen synthase

Merge

10µm

10µm

Merge

10µm
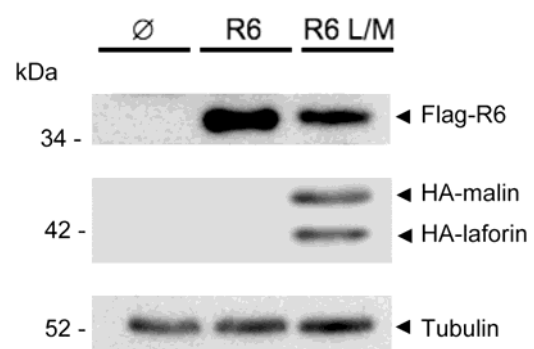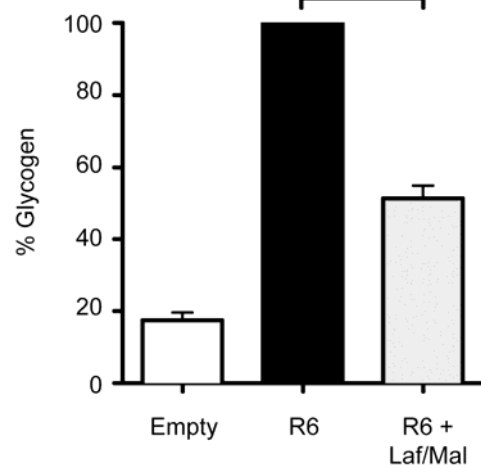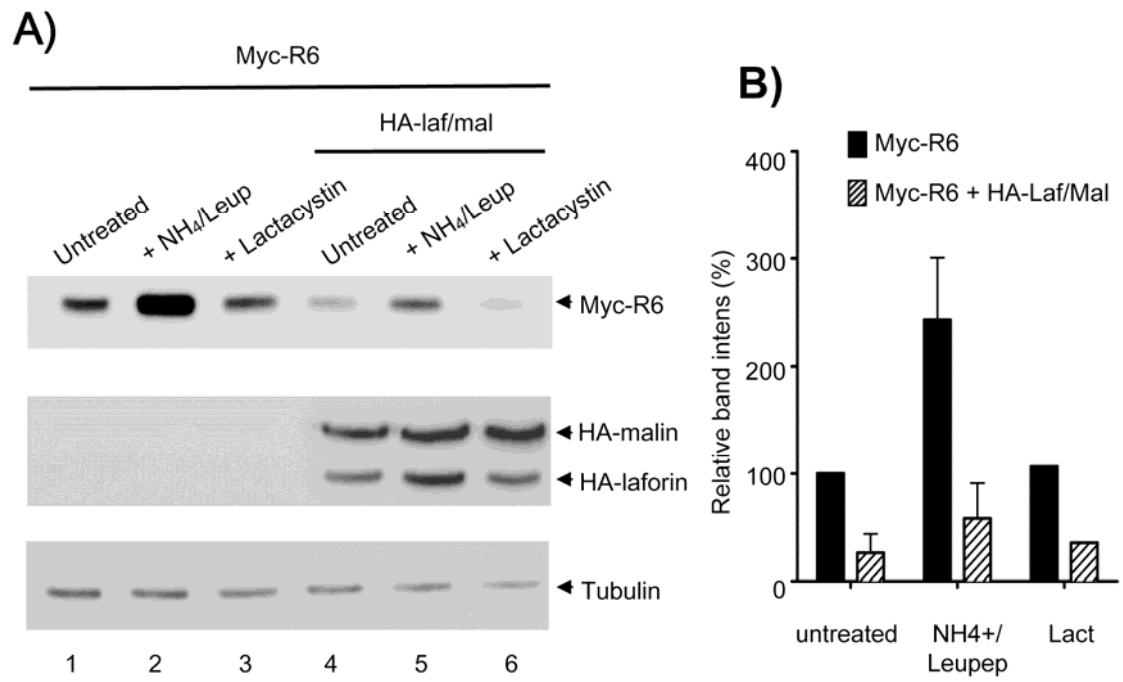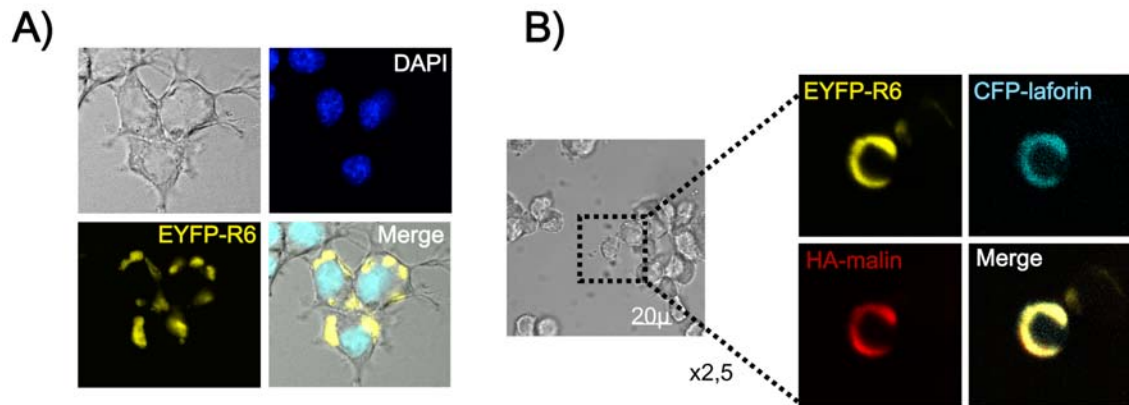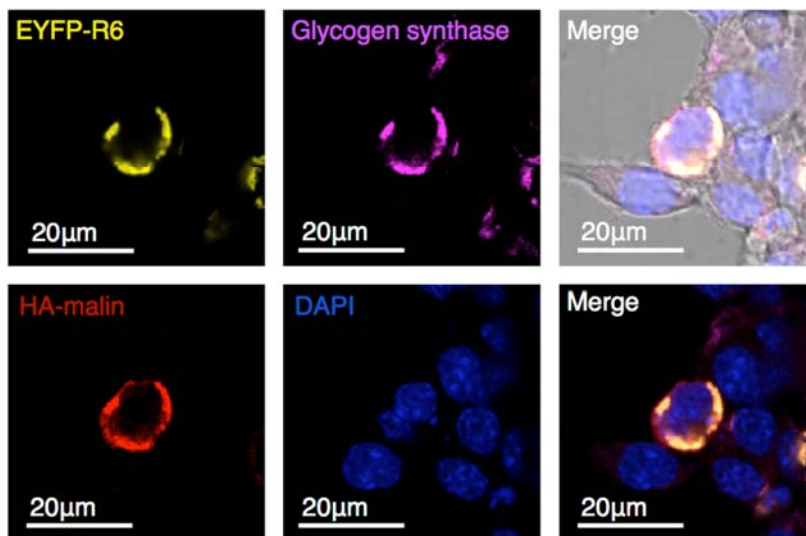
A) siRNA laforin

B) siRNA mock
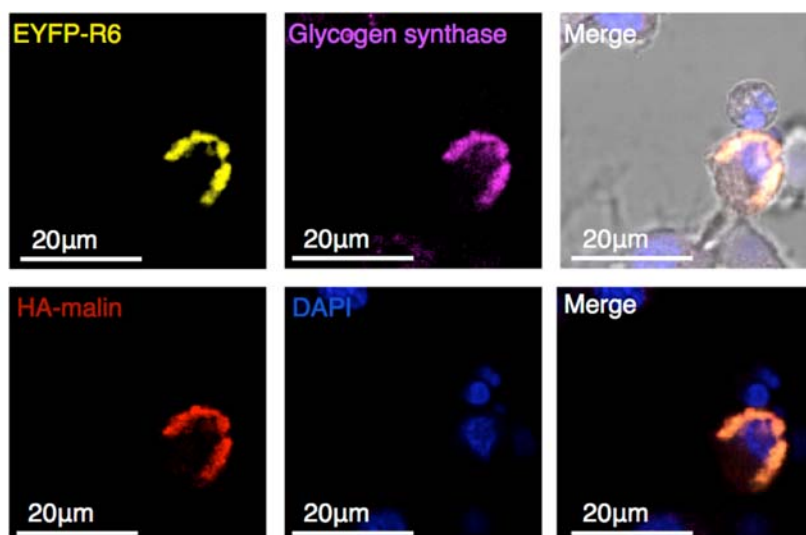
Supplementary Figure S1. Co-localization of R6 (yellow), malin (red) and glycogen synthase (magenta) in N2a cells. A) N2a cells were transfected with Laforin-siRNA (50nM) (OpenBiosystems, Waltham, USA) achieving a 4-fold reduction in laforin gene expression measured by qRT-PCR. After 24h, cells were transfected with pEYFP-R6 and pcDNA3-HA-malin and then treated with DAPI to stain the nucleus. B) Same procedure as in panel A) but using random RNA (mock) as a control. In both cases, endogenous glycogen synthase immunodetection was carried out using anti-glycogen synthase as primary antibody and Alexa-Fluor 633 as secondary antibody. The subcellular localization of EYFP-R6 and HA-malin was carried out as described in Material and Methods. The four images were subjected to merge analysis using the ImageJ 1.43c software.